JCB Article

NuSAP, a novel microtubule-associated protein involved in mitotic spindle organization

Tim Raemaekers,[1] Katharina Ribbeck,[3] Joël Beaudouin,[3] Wim Annaert,[2] Mark Van Camp,[1] Ingrid Stockmans,[1] Nico Smets,[1] Roger Bouillon,[1] Jan Ellenberg,[3] and Geert Carmeliet[1]

[1]Laboratory for Experimental Medicine and Endocrinology and [2]Neuronal Membrane Trafficking Laboratory, Center for Human Genetics/VIB04, Katholieke Universiteit Leuven, B-3000 Leuven, Belgium
[3]Gene Expression and Cell Biology/Biophysics Programs, European Molecular Biology Laboratory (EMBL), D-69117 Heidelberg, Germany

Here, we report on the identification of nucleolar spindle–associated protein (NuSAP), a novel 55-kD vertebrate protein with selective expression in proliferating cells. Its mRNA and protein levels peak at the transition of G2 to mitosis and abruptly decline after cell division. Microscopic analysis of both fixed and live mammalian cells showed that NuSAP is primarily nucleolar in interphase, and localizes prominently to central spindle microtubules during mitosis. Direct interaction of NuSAP with microtubules was demonstrated in vitro. Overexpression of NuSAP caused profound bundling of cytoplasmic microtubules in interphase cells, and this relied on a COOH-terminal microtubule-binding domain. In contrast, depletion of NuSAP by RNA interference resulted in aberrant mitotic spindles, defective chromosome segregation, and cytokinesis. In addition, many NuSAP-depleted interphase cells had deformed nuclei. Both overexpression and knockdown of NuSAP impaired cell proliferation. These results suggest a crucial role for NuSAP in spindle microtubule organization.

Introduction

During cell division, a complete set of duplicated chromosomes must be evenly distributed to two daughter cells. This is accomplished by the mitotic spindle, a bipolar, microtubule-based structure that arises from profound rearrangements of the microtubule network at the start of mitosis. The interphase microtubule network disassembles, and mitotic microtubules reassemble around condensed chromatin and the two centrosomes. Multiple proteins associate with the mitotic spindle and are essential for its assembly and function (for review see Merdes and Cleveland, 1997; Karsenti and Vernos, 2001; Wittmann et al., 2001). These include centrosomal factors such as γ-tubulin (Joshi et al., 1992), as well as proteins that are not directly anchored to the pericentriolar material, such as NuMA and TPX2 (Compton et al., 1992; Yang et al., 1992; Wittmann et al., 2000), dynactin (Gaglio et al., 1997), several microtubule-dependent motor proteins, including dynein (Heald et al., 1996), and the small GTPase, Ran (for review see Kahana and Cleveland, 1999; Hetzer et al., 2002).

NuMA and TPX2 have been identified only in vertebrates and both show a cell cycle–dependent localization, being nuclear during interphase and spindle-associated during mitosis. Ran and the importins, the nuclear transport receptors, regulate NuMA and TPX2 activity, sequestering them from cytoplasmic tubulin until mitotic breakdown of the nuclear envelope (for review see Dasso, 2001; Kahana and Cleveland, 2001). During mitosis, Ran's function in spindle formation has been proposed to rely on elevated concentrations of its GTP-bound form (Ran-GTP) in the vicinity of chromosomes, thereby activating mediators of spindle assembly like NuMA and TPX2 through disassembly of inhibitory importin complexes. This would result in a local environment favorable for microtubule nucleation and stabilization around chromosomes (Gruss et al., 2001; Nachury et al., 2001; Wiese et al., 2001).

The proper assembly and function of the spindle is essential for genomic stability, and therefore, knowledge of key factors involved in this process and their mechanisms of action is crucial. In this paper, we have identified a novel protein, nucleolar spindle–associated protein (Nu-

Address correspondence to Geert Carmeliet, Legendo, Onderwijs & Navorsing, Gasthuisberg, Herestraat 49, B-3000 Leuven, Belgium. Tel.: 32-16-345974. Fax: 32-16-345934. email: geert.carmeliet@med.kuleuven.ac.be

Key words: mitotic spindle apparatus; microtubules; nucleus; mitosis; nucleolus

Abbreviations used in this paper: ChHD, charged helical domain; MAP, microtubule-associated protein; NuSAP, nucleolar spindle–associated protein; siRNA, small interfering RNA.

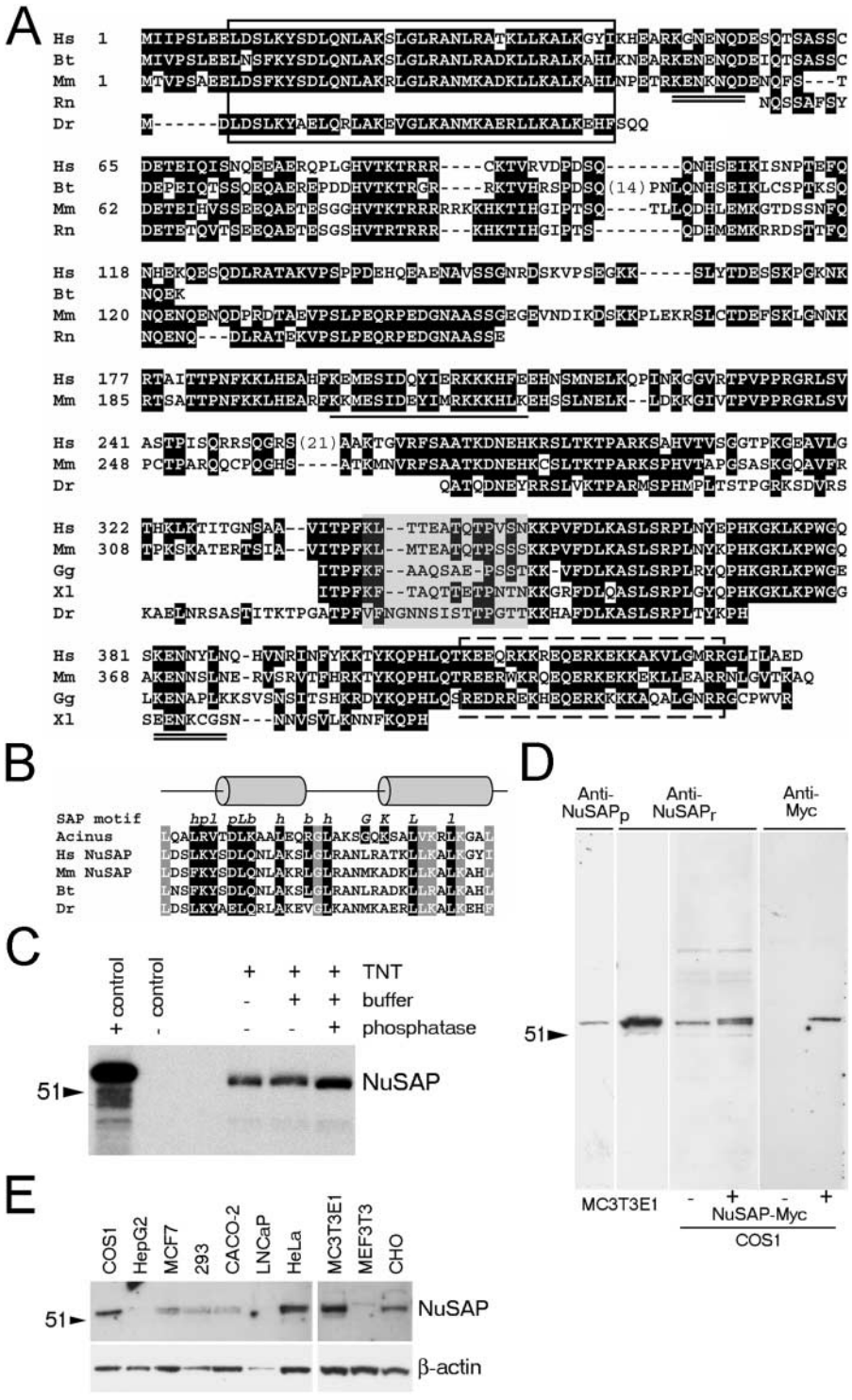

Figure 1. **Identification of NuSAP.** (A and B) Deduced amino acid sequence of mouse and human NuSAP and its alignment with predicted proteins from other species, and with the SAP motif consensus sequence. (A) Identical and similar residues are shaded in black. Homologous residues were taken as follows: positively charged (R and K), negatively charged (E and D), and hydrophobic (L,V,I,F, and M). Gaps, indicated by dashes or numbers between parentheses, were introduced for optimal alignment. Boxed at the NH_2 terminus is the potential SAP motif, and at the COOH terminus (in dashed lines) is a conserved stretch of highly charged residues, with a predicted helical structure, which we have named the ChHD domain. The potential PEST sequence is shaded in gray, and the putative KEN boxes are double underlined. The potential NLS identified in the mouse sequence is underlined. (B) Residues within the SAP motif consensus sequence have been defined by Aravind and Koonin (2000): *h* (hydrophobic), *p* (polar), *l* (aliphatic), and *b* (bulky). Also shown is the sequence of Acinus (GenBank/EMBL/ DDBJ accession no. AAF89661), a SAP module–containing protein. Shaded in black are residues that agree with the consensus sequence, and in gray are residues that conform to the similarity as described in A. Sequences besides those of mouse and human were deduced from ESTs. The GenBank/EMBL/DDBJ accession nos. are as follows: Hs, *Homo sapiens* (AAG25874); Bt, *Bos taurus* (BE480183); Mm, *Mus musculus* (AAG31285); Rn, *Rattus norvegicus* (AA923940); Gg, *Gallus gallus* (AJ392813); Xl, *Xenopus laevis* (AW642384); and Dr, *Danio rerio* (AI545826, AI958745). (C) SDS-PAGE of radiolabeled, in vitro transcribed and translated NuSAP. The transcription and translation reaction (TNT) was followed by treatment of the sample with calf intestine alkaline phosphatase buffer in the absence (buffer) or presence of (phosphatase) enzyme. The bandshift indicates that in vitro–produced NuSAP is a phosphoprotein. Luciferase DNA was used as a positive control, whereas no DNA template was used in the negative control. (D) Western blot of total cell lysates prepared from MC3T3E1 cells and transfected COS1 cells. For transfections, an empty control or NuSAP-Myc vector was used. The blot was probed for NuSAP expression using both anti-NuSAP and anti-Myc antibodies. The polyclonal anti-NuSAP antibodies include an anti-peptide (Anti-$NuSAP_p$) and an anti-recombinant protein (Anti-$NuSAP_r$) antibody. (E) Western blot analysis for NuSAP expression in different cell lines. The blot, which was prepared from total cell lysates, was also probed for β-actin expression. Arrowhead indicates the 51-kD marker (C–E).

SAP), which is well conserved in vertebrates, and shows a cell cycle–dependent localization and microtubule-binding properties similar to NuMA and TPX2. Interestingly, NuSAP specifically associates with spindle microtubules in close contact with chromosomes in metaphase/anaphase. Depletion of NuSAP from cells by RNA interference results in evident mitotic defects that interfere with normal cell cycle progression.

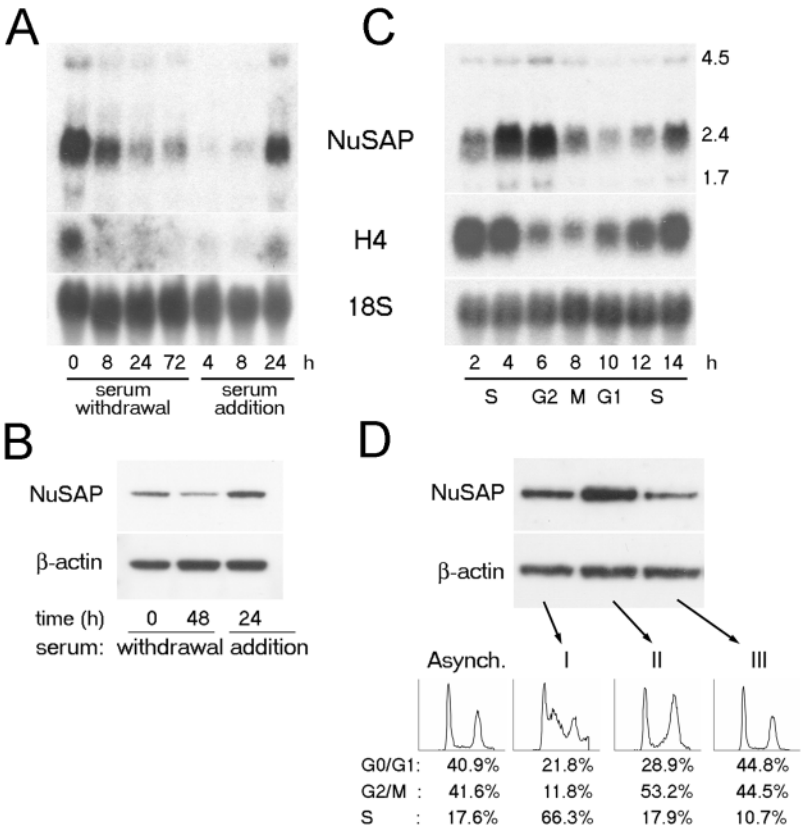

Figure 2. **NuSAP expression is up-regulated in proliferating cells during G2/M phase of the cell cycle.** (A–D) Northern and Western blot analysis for NuSAP expression in synchronized MC3T3E1 cells. RNA or protein was isolated at the indicated time points (h). (A and B) Cells were arrested in their growth by serum starvation, and subsequently released by addition of complete medium. (C and D) Cells were synchronized using a double-thymidine block. (D) DNA content of thymidine-synchronized cells was determined by FACS® analysis at time points I–III. (A and C) Northern blots were also probed for *histone H4* expression, an S phase marker. *NuSAP* transcript sizes (kb) are indicated. As a loading control, blots were probed for 18S or β-actin expression.

Results

Identification of NuSAP as a proliferation marker

We compared gene expression patterns of proliferating and differentiating mouse MC3T3E1 osteoblasts by differential display, and identified a cDNA fragment that showed enhanced levels during proliferation. The full-length mouse sequence of this transcript contained a single ORF of a 1,281-bp coding region, which is identical to the sequence of an uncharacterized lymphocyte protein (GenBank/EMBL/DDBJ accession no. AAG31285). The protein was designated NuSAP (see following paragraphs). Cloning of the human *NuSAP* cDNA and comparison with EST databases showed that NuSAP is highly conserved in vertebrates, but no clear homologues could be identified in invertebrates (Fig. 1 A). Mouse *NuSAP* cDNA is predicted to encode a protein of 427 aa with a calculated molecular mass of 48.6 kD and an isoelectric point of 9.9. The apparent molecular mass of NuSAP was slightly higher, being ~55 kD (Fig. 1 C), and this difference can be partially accounted for by phosphorylation as shown by treatment with alkaline phosphatase (Fig. 1 C), but appears to be primarily the result of the high basicity of the protein.

Mouse NuSAP contains a potential bipartite NLS within a predicted helical domain that is conserved between mice and humans. In addition, a 35-aa region at the NH_2 terminus is a potential SAP motif, a helix–extension–helix domain that has been described to interact with DNA and to be involved in chromosomal organization (Aravind and Koonin, 2000; Fig. 1, A and B). Furthermore, NuSAP appears to contain several consensus phosphorylation sites for casein kinase II and PKC, as well as three consensus sites for mitotic cdc2 kinase (Peter et al., 1990). Sequence alignments of the NuSAP protein from different species indicated the presence of a potential KEN box (Pfleger and Kirschner, 2000) and PEST sequence (Rechsteiner and Rogers, 1996) toward the COOH terminus of NuSAP (Fig. 1 A). A second less conserved KEN box may reside more NH_2 terminally (Fig. 1 A). At the very COOH terminus, NuSAP contains an exceptionally highly charged domain with a predicted helical structure that is well conserved between species. Therefore, we have named this novel domain as charged helical domain (ChHD; Fig. 1 A).

To characterize NuSAP further, we generated pAbs against a peptide (anti-$NuSAP_p$) and recombinant protein (anti-$NuSAP_r$). These antibodies specifically recognized the endogenous protein in MC3T3E1 cells and other cell lines of mouse, hamster, monkey, and human origin, as well as endogenous and epitope-tagged NuSAP expressed in COS1 cells (Fig. 1, D and E).

NuSAP expression is up-regulated during the G2/M phase of the cell cycle

To confirm the initial observation that *NuSAP* expression is proliferation related, MC3T3E1 cells were specifically arrested in their growth by serum withdrawal and analyzed for *NuSAP* expression by Northern blot analysis. An ~2.4-kb band was identified as the major transcript, and as expected, *NuSAP* RNA levels were reduced more than 10-fold. When quiescent cells were resupplemented with serum, *NuSAP* RNA levels increased again, displaying an expression pattern

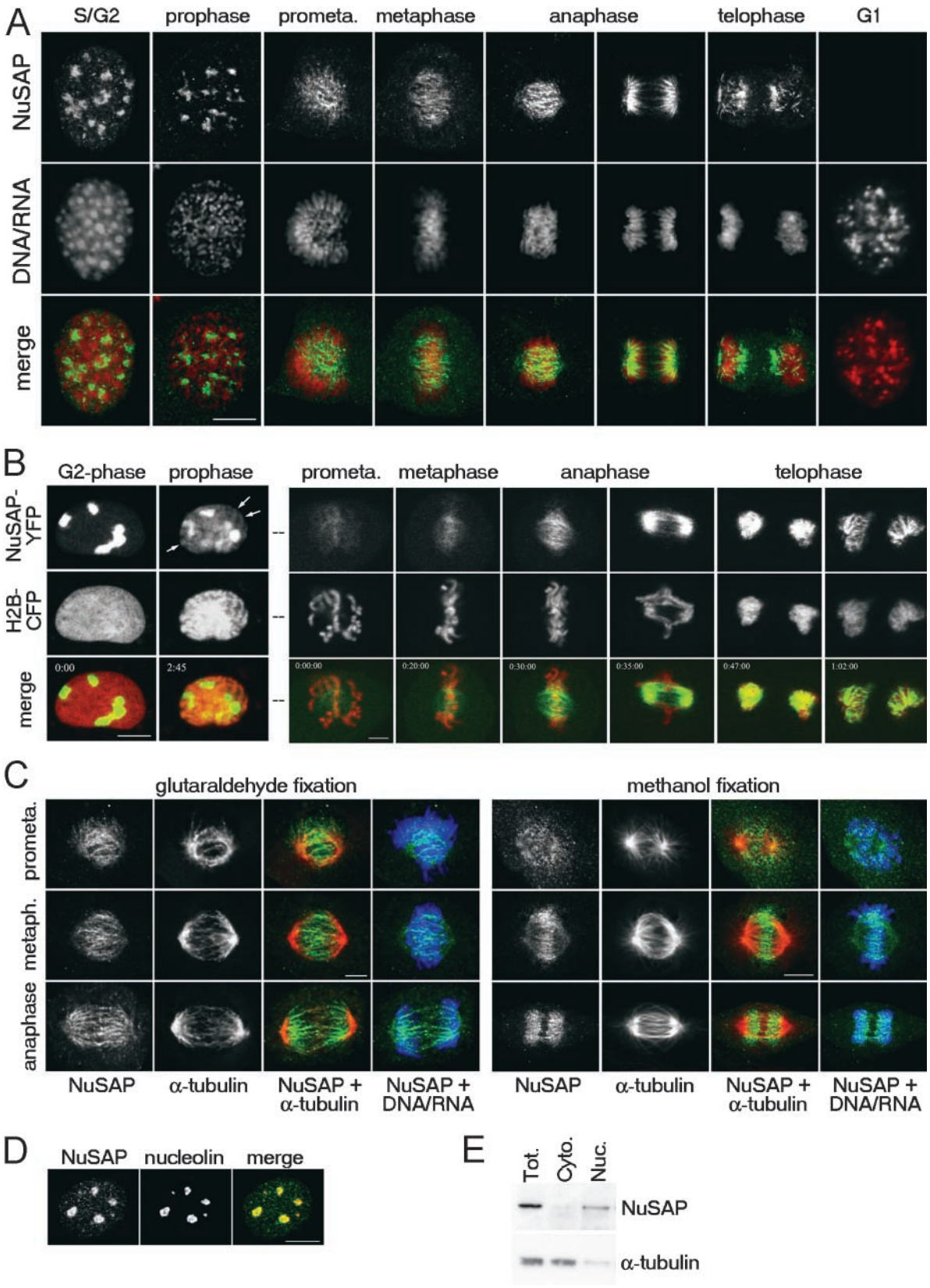

Figure 3. **Dynamic localization of NuSAP during the cell cycle.** (A) Synchronized MC3T3E1 cells were fixed at specific time points, and double stained for endogenous NuSAP and nucleic acids. NuSAP is nuclear at S/G2 phases. During metaphase and early anaphase, NuSAP localizes prominently to the central spindle. Toward the end of cytokinesis and in G1 phase, NuSAP is hardly detectable. (B) Time-lapse microscopy of synchronized, live NRK cells stably expressing CFP-tagged histone 2B (H2B-CFP) and transiently expressing YFP-tagged NuSAP. In vivo images show a similar subcellular localization as with fixed cells. Arrows indicate association with condensing chromosomes at prophase. Time is h:min:s. (C) Double-stained MC3T3E1 cells (endogenous NuSAP and α-tubulin, or nucleic acids) were fixed in either

similar to the growth marker *histone H4* (Stein et al., 1990b; Fig. 2 A). At the protein level, NuSAP expression was reduced more than threefold, 48 h after serum withdrawal, and increased again in cells that subsequently resumed growth (Fig. 2 B).

A more detailed analysis of *NuSAP* gene expression throughout the cell cycle using synchronized MC3T3E1 cells revealed that the gene is highly transcribed in late S/G2 phase of the cycle with very low expression levels (more than eightfold reduction) in G1 phase (Fig. 2 C). Western blot analysis of synchronized cells showed highest protein levels in the G2/M phase (Fig. 2 D).

Cell cycle–dependent localization of NuSAP to the nucleus and mitotic spindle

The subcellular distribution of NuSAP was followed throughout the cell cycle by immunostaining and in vivo imaging. Immunofluorescence microscopy of MC3T3E1 cells revealed that during interphase, endogenous NuSAP was confined to the nucleus and concentrated in nucleoli (Fig. 3 A, S/G2; Fig. 3 D). Cell fractionation experiments confirmed this nuclear localization (Fig. 3 E). At prometaphase, NuSAP redistributed from nucleoli to the vicinity of the chromosomes, forming bundles that became progressively more defined at metaphase and early anaphase (Fig. 3 A). These NuSAP bundles colocalized with microtubules of the central spindle (Fig. 3 C). Later in anaphase, NuSAP was intensely localized to the spindle in the chromosomal area. At telophase, NuSAP localized to "spikes" around the decondensing chromosomes, which disappeared toward the end of cytokinesis (Fig. 3 A). Consistent with the reduced protein levels in G1 cells seen by Western blot (Fig. 2 D), very little NuSAP could be detected in G1 cells (Fig. 3 A), indicating a rapid degradation of NuSAP after mitosis. Interestingly, the localization of NuSAP to chromosomes in mitotic cells was not sensitive to nocodazole treatment, indicating that part of its mitotic localization may be independent of microtubules (unpublished data).

To confirm the antibody staining that yielded slightly different results depending on the fixation method used (Fig. 3 C), we next examined the dynamic localization of NuSAP tagged with YFP in live NRK cells (stably expressing histone 2B-CFP). Very similar to the immunofluorescence data, in interphase, NuSAP localized to the nucleus, being highly enriched in the nucleoli (Fig. 3 B). At prophase, NuSAP was primarily nucleolar; however, a small fraction associated with condensing chromosomes (Fig. 3 B, arrows). Concomitant with nuclear envelope breakdown in prometaphase, a large fraction of NuSAP was released as a soluble pool in the cytoplasm, but some started to localize to bundles in the central spindle region that accumulated more and more NuSAP until anaphase, thereby depleting the soluble pool (Fig. 3 B). In late anaphase, soluble NuSAP was barely detectable, and all of NuSAP was localized in thick bundles around chromosomes that were transformed to the characteristic NuSAP spikes in telophase (Fig. 3 B) before the protein was degraded in G1 (unpublished data). Based on the localization of NuSAP to the nucleolus during interphase, and to the spindle during mitosis, we have named the protein NuSAP, for nucleolar spindle–associated protein.

NuSAP is a microtubule-associated protein (MAP)

NuSAP's specific localization to central spindle microtubules in mitotic cells led us to study whether it interacts with pure prepolymerized microtubules in a sedimentation assay. First, we used in vitro translated NuSAP in the assay, and as shown in Fig. 4 A, NuSAP was recovered in the microtubule pellet when microtubules were present, but remained soluble in the absence of microtubules (Fig. 4 A). This interaction was specific, as a well-characterized MAP (MAP2) also bound to microtubules, whereas BSA did not (unpublished data). To estimate the affinity of NuSAP for microtubules, NuSAP was mixed with different concentrations of microtubules in the same assay. Plotting of bound NuSAP versus the microtubule concentration and direct hyperbolic curve-fitting yielded an equilibrium dissociation constant of $\sim$1 μM (the tubulin concentration required to bind 50% of NuSAP; Fig. 4 B), indicating microtubule binding with moderately high affinity. To determine whether NuSAP interacts directly with microtubules, the sedimentation assay was repeated in a more defined system using purified recombinant NuSAP protein and pure prepolymerized microtubules. Recombinant NuSAP copelleted to large parts with microtubules, and only little remained in the microtubule-unbound supernatant fraction (Fig. 4 C). These results indicate that NuSAP not only colocalizes, but also directly binds to microtubules, fulfilling the criteria of a bona fide MAP.

Nuclear NuSAP can bind cytoplasmic microtubules via a COOH-terminal domain

In interphase cells, NuSAP was primarily localized to the nucleolus, but at the onset of mitosis, NuSAP was released from the nucleus and associated with a subset of spindle microtubules. To determine whether nuclear NuSAP is competent to bind cytoplasmic microtubules during interphase, we permeabilized the nuclear envelope of MC3T3E1 cells by brief incubation in detergent before fixation to allow passage of NuSAP into the cytoplasm. Under these conditions, nucleolar staining was markedly reduced and NuSAP redistributed to a perinuclear microtubule network as shown by colocalization with α-tubulin (Fig. 4 D). This localization was dependent on microtubule integrity, as it was no longer present after nocodazole or cold treatment (unpublished data). For comparison, the mitotic MAP, NuMA (Compton

glutaraldehyde or methanol. Methanol-fixed cells showed intact spindle microtubules, whereas NuSAP integrity is impaired. In contrast, cells fixed in detergent-containing glutaraldehyde solution showed more integer NuSAP, whereas microtubule integrity was affected. (D) MC3T3E1 cells at interphase were double stained for endogenous NuSAP and nucleolin. NuSAP is highly enriched in the nucleolus. (A and D) Mitotic cells were fixed in glutaraldehyde, whereas PFA was used for interphase cells. (E) Western blot of total cell lysate and cytosol and nuclear fractions of MC3T3E1 cells. The blot was probed with anti-NuSAP and anti-α-tubulin antibodies. In contrast to tubulin, NuSAP is primarily recovered in the nuclear fraction. Bars: (A and D) 10 μm; (B and C) 5 μm.

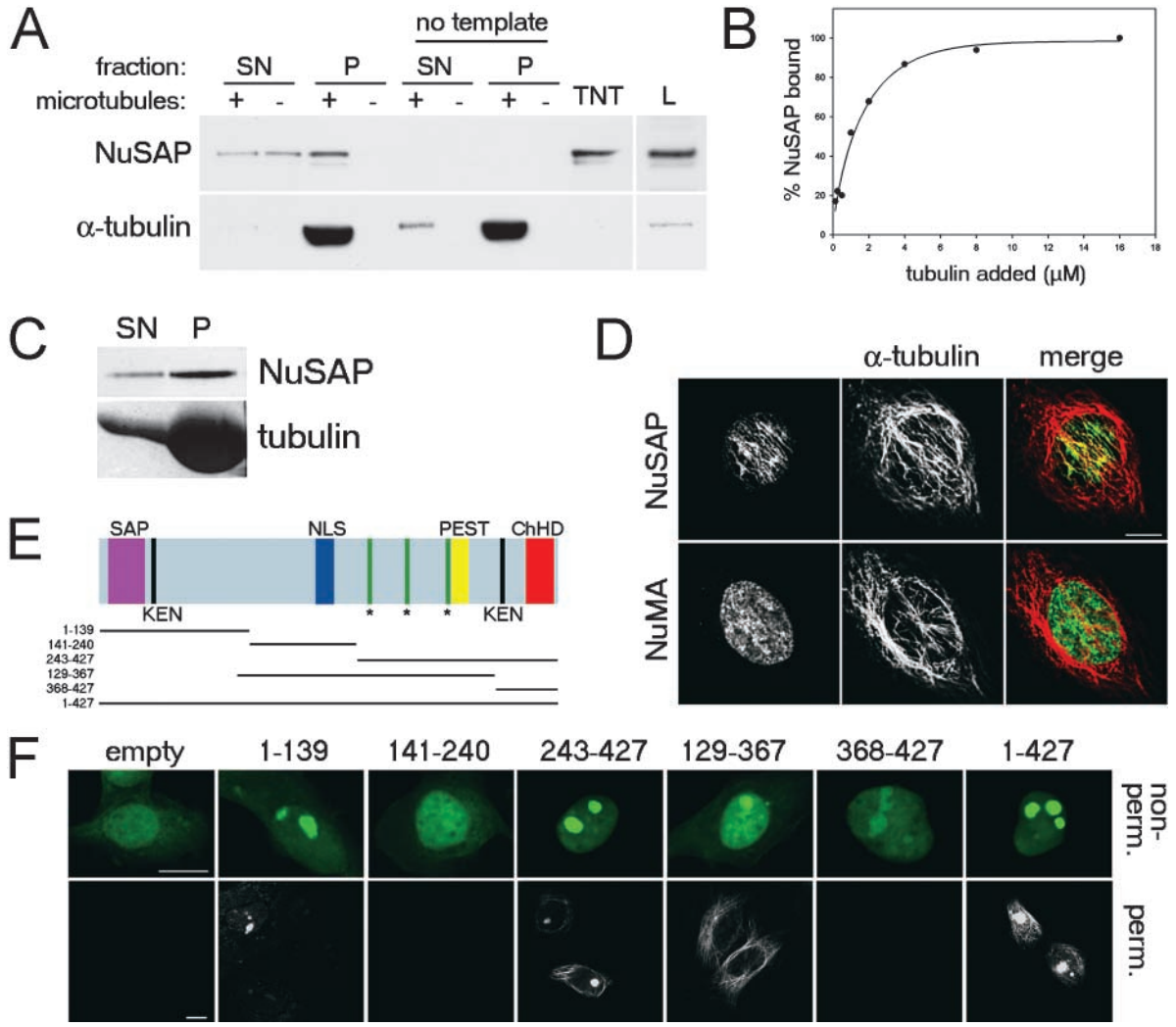

Figure 4. **NuSAP binds to microtubules in vitro and in vivo.** (A and B) Microtubule sedimentation assay of in vitro produced NuSAP with pure prepolymerized microtubules. (A) The assay was performed using crude in vitro translation product in the presence (+) or absence (−) of microtubules. Recovery of NuSAP in the microtubule pellet (P) fraction, as opposed to the soluble supernatant (SN) fraction, was determined by immunoblotting with anti-NuSAP and anti-α-tubulin antibodies. As a negative control, the assay was performed using reaction product with no template DNA. Included on the blot is an in vitro transcription and translation product of NuSAP (TNT) and total cell lysate prepared from MC3T3E1 cells (L). (B) Affinity of NuSAP for microtubules was determined by plotting bound NuSAP versus the tubulin concentration yielding a dissociation constant (Kd) of ~1 μM. (C) Microtubule sedimentation assay with purified recombinant NuSAP (detected by Western blot) and pure prepolymerized microtubules (Coomassie). (D) Interphase MC3T3E1 cells were briefly permeabilized before PFA fixation, and double stained for α-tubulin and endogenous NuSAP or NuMA. NuSAP (but not NuMA) colocalizes to perinuclear microtubules. (E and F) Full-length and various GFP-tagged NuSAP fragments were analyzed in transfected COS1 cells for subcellular localization and microtubule-binding potential. In the latter assay, cells were permeabilized (perm.) before glutaraldehyde fixation. The microtubule-binding domain of NuSAP lies toward the COOH terminus, as fragments 243–427 and 129–367, like full-length NuSAP, associates with microtubules. For subcellular localization studies, nonpermeabilized cells (nonperm.) were fixed in PFA. Bars: (D and F) 10 μm.

et al., 1992; Yang et al., 1992; Haren and Merdes, 2002), which shows a cell cycle distribution similar to NuSAP, remained nuclear under the same conditions (Fig. 4 D).

The region within NuSAP that mediates binding to microtubules was determined using the permeabilization/fixation assay described above. A series of GFP-tagged NuSAP fragments were expressed in COS1 cells (Fig. 4, E and F) and assayed for binding to cytoplasmic microtubules after permeabilization. First, however, the intracellular distribution of the various NuSAP fragments was analyzed in nonpermeabilizing conditions. As shown in Fig. 4 F, all NuSAP fragments localized to the nucleus in interphase, and some showed a prominent nucleolar staining as observed for full-length NuSAP (for a detailed summary, see Table I). In permeabilized cells, only NuSAP fragments 243–427 and 129–367 showed localization to cytoplasmic microtubules similar to full length NuSAP. Thus, the minimal microtubule-binding domain is contained toward the COOH terminus of NuSAP, between residues 243–367 (Fig. 4 E).

Overexpression of NuSAP causes bundling of cytoplasmic microtubules

To study the effect of gain of NuSAP function, full-length and various fragments of GFP-tagged NuSAP were overex-

Table I. **Subcellular distribution of full-length and various GFP-tagged NuSAP fragments in (non)permeabilized cells**

Construct	Subcellular localization			Localization after permeabilization			Microtubule bundling
	Cytoplasm	Nucleus	Nucleolus	Microtubules	Nucleus	Nucleolus	
1–139	+	++	+++	-	+	++	-
141–240	+	++	+	-	-	-	-
243–427	-	++++	+++++	++	++	+++	+
129–367	+	++	++	+++	+	+	+
368–427	-	++++	+	-	-	-	-
1–427	-	++++	+++++	++	++	+++	+
Empty	++	+	-	-	-	-	-

Presence and intensity of GFP fluorescence is indicated together with the microtubule-bundling potential of the different fusion proteins.

pressed in COS1 cells, and their effects on the microtubule network were analyzed by (immuno)fluorescence microscopy. Overexpression of full-length NuSAP protein resulted in the appearance of long, curved, and unusually thick microtubule bundles in the cytoplasm, to which NuSAP colocalized. These bundled microtubules were extremely stable, and did not depolymerize in the presence of high doses of nocodazole (Fig. 5 A). Similarly, overexpression of the NuSAP fragments 243–427 and 129–367 (Table I) caused strong bundling of cytoplasmic microtubules, confirming their microtubule-binding competence.

To determine how the NuSAP-induced microtubule bundles arise, we performed time-lapse microscopy of PtK_2 cells that stably express YFP-tagged α-tubulin and had been transfected with CFP-tagged NuSAP (Fig. 5 B). As the amount of NuSAP increased, the nuclear fraction appeared to saturate, and cytoplasmic NuSAP became detectable and immediately colocalized with microtubules (Fig. 5 B, 4:30–6:30). Increasing amounts of NuSAP in the cytoplasm resulted in the rearrangement of the microtubule network with formation of large bundles within minutes (Fig. 5 B, 8:20). These profound effects of NuSAP overexpression ultimately led to clear changes in cellular morphology, growth arrest, and affected viability. To confirm the effect on viability, GFP-tagged NuSAP was expressed in proliferating HeLa cells, and the percentage of GFP-expressing cells was counted at 24, 48, and 72 h after transfection. Although the number of GFP-transfected cells decreased only slightly with time (89% expressing GFP, 72 h after transfection), the percentage of NuSAP-GFP–expressing cells dropped to 18% at 72 h after transfection.

Suppression of NuSAP by small interfering RNA (siRNA) causes delayed entry into mitosis

To study the effect of loss of NuSAP function, NuSAP protein levels were suppressed in HeLa cells using siRNA duplexes (Elbashir et al., 2001). Immunoblot and immunofluorescence analysis showed that at 24 h after transfection, the level of endogenous NuSAP could be reduced by more than ninefold in cells transfected with duplexes directed to Nu-

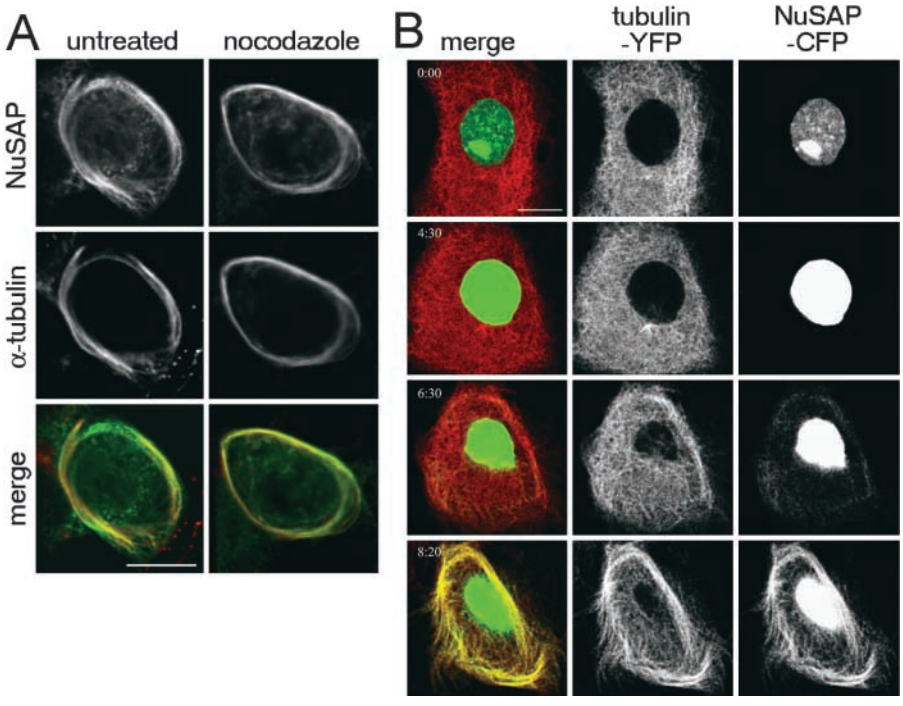

Figure 5. **Overexpression of NuSAP caused bundling of cytoplasmic microtubules.** (A) Myc-tagged full-length NuSAP was analyzed in interphase COS1 cells 24 h after transfection. Cells were fixed in glutaraldehyde and double stained for Myc-tagged NuSAP and α-tubulin. NuSAP overexpression induces microtubule bundles that resist nocodazole treatment. (B) Time-lapse microscopy of a PtK_2 cell stably expressing YFP-tagged α-tubulin and transiently expressing CFP-tagged NuSAP. NuSAP overexpression leads to a cytoplasmic pool of NuSAP with subsequent bundling of microtubules. Time is h:min. Bars: (A and B) 10 μm.

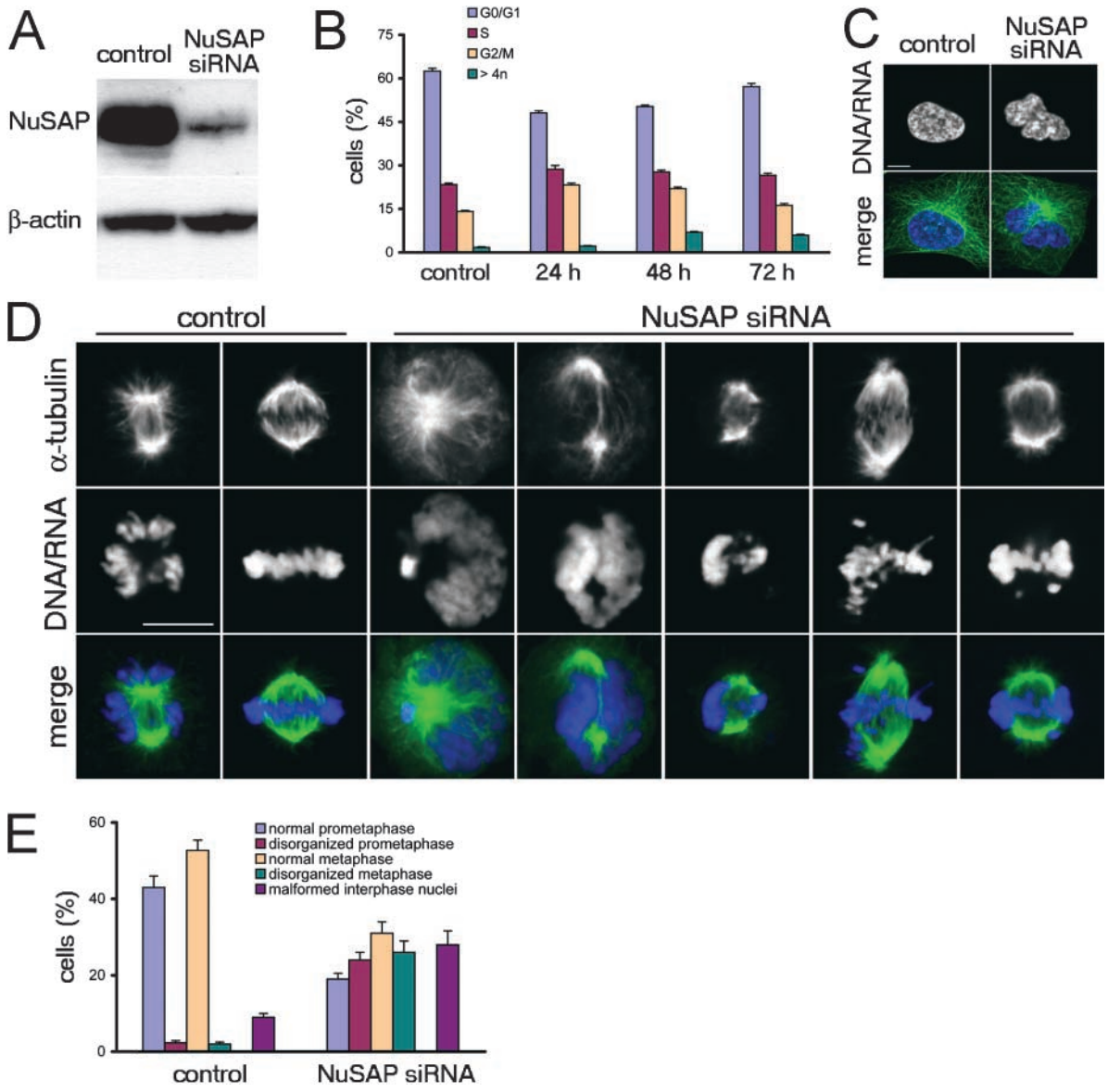

Figure 6. **Suppression of NuSAP by siRNA causes delayed entry into mitosis.** (A–E) HeLa cells were analyzed at specific time points after transfection with either control or NuSAP-specific siRNA duplexes. (A) Western blot of total cell lysates (harvested 24 h after transfection) was probed with antibodies against NuSAP and β-actin (loading control). (B) Time course of change in cellular DNA content after transfection. Quantification also includes the percentage of cells with a larger than tetraploid (4n) DNA content. Data are derived from three independent experiments. (C) Interphase cells 20 h after transfection were fixed in methanol and double stained for α-tubulin (green) and nucleic acids (blue). Abnormally shaped nuclei were observed in NuSAP-suppressed cells. (D) Prometaphase and metaphase spindle appearance in synchronized cells 30 h after transfection (first mitosis with manifest NuSAP suppression). Cells were fixed in methanol and double stained for α-tubulin and nucleic acids. (E) Quantification of the observed abnormal spindle and nuclear phenotypes. For spindles, 100 cells in prometaphase or metaphase from each of three independent experiments were scored for normal or disorganized phenotype. For nuclei, 200 interphase cells from each of three independent experiments were scored for normal or malformed phenotype. Bars: (C and D) 10 μm.

SAP compared with control cells, which were transfected with the nonspecific duplex (transfection efficiencies were typically ~80%; Fig. 6 A; unpublished data).

First, we examined the cell cycle profile of HeLa cells at various time points after depletion of NuSAP. Flow cytometry of DNA content showed an enrichment of cells in G2/M phases, at 24 and 48 h after transfection (>50% increase relative to control cells, Fig. 6 B). Second, we assayed the organization of the mitotic spindle and chromosomes in synchronized HeLa cells 30 h after transfection, at a time when the cells had completed at most one cell cycle with suppressed NuSAP levels. Immunofluorescence showed dramatic mitotic defects (Fig. 6 D). The microtubule organization of prometaphase spindles was abnormal, and frequently associated with an altered condensation pattern of chromosomes. Metaphase cells similarly showed disorganized and less dense arrays of spindle microtubules that were often accompanied by chromosome alignment defects. Approximately 50% of NuSAP-depleted mitotic cells showed either a defect in metaphase or prometaphase (n = 100, three in-

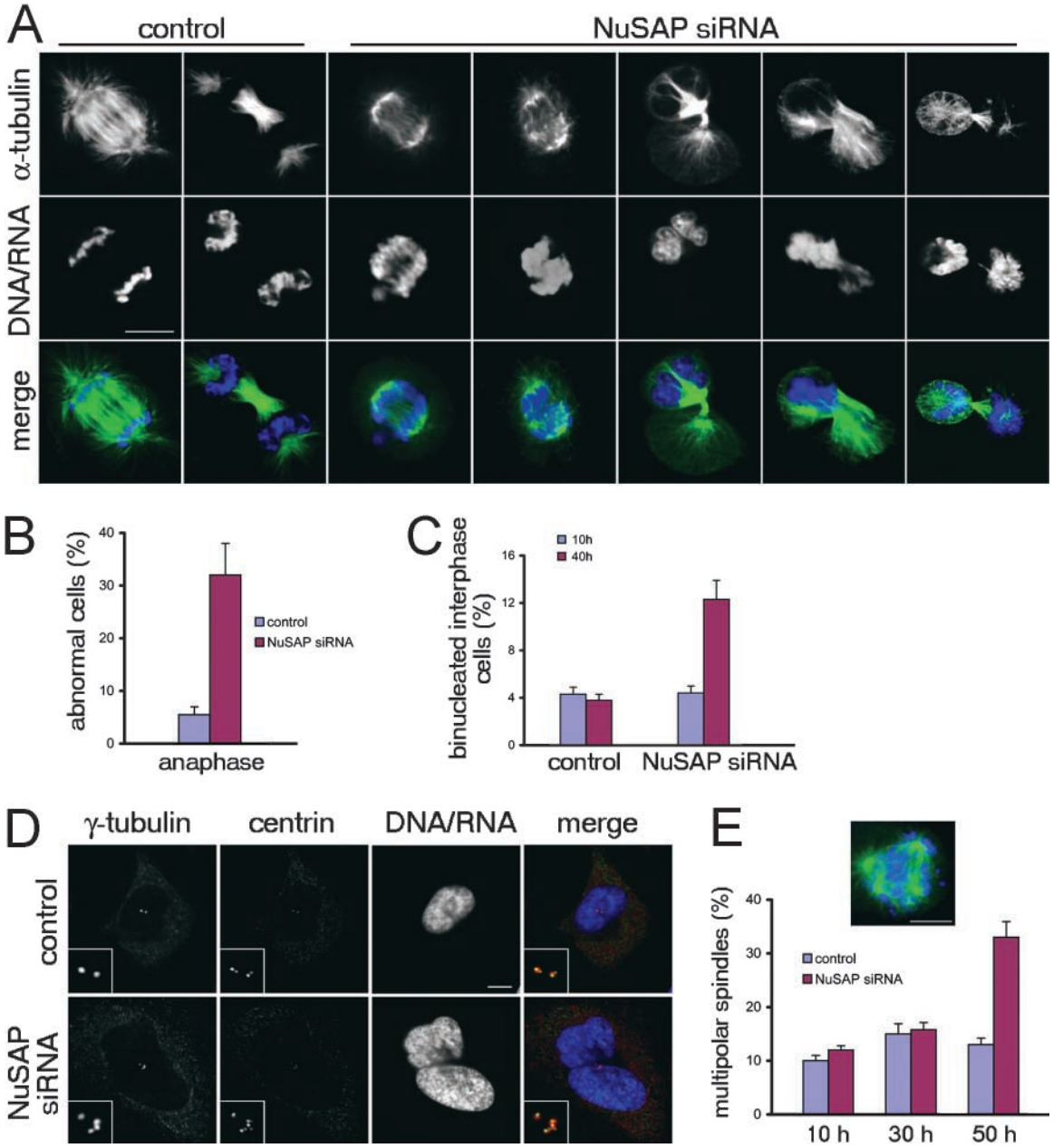

Figure 7. **Suppression of NuSAP results in defective anaphase and cytokinesis.** (A–E) HeLa cells were analyzed at specific time points after transfection with siRNA duplexes. (A) Anaphase and cytokinesis appearance in synchronized cells 30 h after transfection. Cells were fixed in methanol and double stained for α-tubulin and nucleic acids. (B) Quantification of the observed abnormal anaphase spindles. The percentage of normal and abnormal anaphase spindles is depicted with the total anaphase fraction set as 100% (three independent experiments). (C). Relative number of binucleated cells 10 and 40 h after transfection; 300 interphase cells from each of three independent experiments were scored for normal or binucleate phenotype. (D) Cells were fixed in methanol and stained for γ-tubulin, centrin, and nucleic acids 48 h after transfection. Some centrin foci are not clearly visible, as the image was taken at a specific z-axis section. Insets show a higher magnigfication of γ-tubulin and centrin foci. (E) Quantification of the multipolar spindle phenotype in synchronized cells at the indicated time points corresponding to successive mitosis; 100 mitotic cells from each of three independent experiments were scored for the presence of multipolar spindles. Bars: (A, D, and E) 10 μm.

dependent experiments; Fig. 6, D and E). However, some cells appeared to develop normal mitotic spindles despite efficient NuSAP suppression as judged by antibody staining (unpublished data).

Interestingly, suppression of NuSAP also altered nuclear morphology of nondividing HeLa cells (Fig. 6 C) already after 24 h transfection. Staining for nucleic acids (Fig. 6 C) and B-type lamins (unpublished data) revealed that nuclei of depleted cells were frequently folded or invaginated (28% compared with 9% in controls; $n = 200$, three independent experiments; Fig. 6 E).

Suppression of NuSAP results in defective anaphase and cytokinesis

Some of the NuSAP-depleted mitotic cells with highly disorganized spindles appeared to be able to proceed to chro-

mosome segregation. A more than threefold increase in abnormal anaphase cells was observed (n = 100, three independent experiments; Fig. 7, A and B). Again, these cells showed a less dense and disorganized microtubule array, often with aberrant segregation of less condensed chromosomes. At later stages, cells often displayed defective cytokinesis with both chromosome sets in one daughter cell (Fig. 7 A). Consistent with this, we observed a threefold higher number of binucleated cells 40 h after transfection relative to control cells (n = 300, three independent experiments; Fig. 7 C). These cells frequently contained four centrosomes, each containing a pair of centrioles as determined by centrin staining (Fig. 7 D). 50 h after transfection, a time sufficient for cells to complete two cell cycles with reduced levels of NuSAP, we observed a more than threefold increase in the number of multipolar spindles compared with control cells (n = 100, three independent experiments; Fig. 7 E). This agrees well with the increase in binucleated cells at 40 h, and was confirmed by DNA content analysis, which showed a more than threefold increase in cells with a larger than tetraploid DNA content (particularly 6N and 8N DNA content) at both 48 and 72 h after transfection (Fig. 6 B; unpublished data). 72 h after transfection, we could also detect an increase of hypodiploid cells, indicating that NuSAP-depleted cells eventually became apoptotic (unpublished data).

Discussion

NuSAP is a novel mitotic MAP

The cell cycle–dependent subcellular localization of NuSAP is similar to that of other mitotic MAPs, including TPX2 and NuMA (Compton et al., 1992; Yang et al., 1992; Wittmann et al., 2000; Garrett et al., 2002; Gruss et al., 2002). Like these MAPs, NuSAP binds to microtubules via a domain close to its COOH terminus. However, this domain shows no sequence homology with the microtubule-binding domain of other known MAPs, including the tau-like microtubule-binding motif (Drewes et al., 1998). The induction of nocodazole-resistant microtubule bundles by overexpression of NuSAP or its microtubule-binding domain suggests that NuSAP has a stabilizing effect on microtubules, similar to that described for the cytoplasmic MAPs tau and MAP2 (Lewis et al., 1989; Takemura et al., 1992), and more recently for the mitotic MAPs NuMA and TPX2 (Gruss et al., 2002; Haren and Merdes, 2002). However, NuSAP does distinguish itself from other mitotic MAPs by its prominent central spindle microtubule localization during metaphase and early anaphase. This was shown for both the endogenous protein and when YFP-tagged NuSAP was expressed at low levels, and may indicate a function in stabilizing chromosome-associated microtubules.

Sequestration of NuSAP to the nucleus during interphase prevents any interactions with microtubules until after breakdown of the nuclear membrane, at the beginning of mitosis. The localization and activity of NuSAP could be regulated in a similar manner as NuMA and TPX2, where nuclear localization is governed by asymmetric distribution of the GTPase Ran, and binding to the nuclear transport receptors, importin-α and -β (for review see Dasso, 2001; Kahana and Cleveland, 2001). NuSAP could interact with nuclear transport receptors via the two different domains that were sufficient for nuclear targeting. The first is the potential bipartite NLS, which could interact with importin-α and -β. Interestingly, the novel ChHD also conferred nuclear localization. It has recently been suggested that importins might act as chaperones for exposed basic domains (Jakel et al., 2002), and ChHD is extremely basic with an isoelectric point >10. Thus, importins might bind to this region, stabilizing an inactive state by shielding of basic patches, and simultaneously might import NuSAP into the nucleus.

NuSAP is a cycling protein essential for cell cycle progression

Protein levels of NuSAP were cell cycle regulated and restricted to late S/G2 and M phases with undetectable expression in G1, similar to the expression pattern of human TPX2 (Heidebrecht et al., 1997; Gruss et al., 2002). Although the increased expression in late S phase correlated well with transcription levels, the rapid disappearance of the protein in G1 suggests rapid degradation after cytokinesis. This is consistent with the potential KEN boxes and PEST sequence in NuSAP, which could target NuSAP to the ubiquitin/proteasome pathway (Rechsteiner and Rogers, 1996; Pfleger and Kirschner, 2000). This destruction may be important for proper exit from mitosis, to prevent any excess NuSAP from associating and bundling cytoplasmic microtubules in interphase. Consistent with this, increased levels of NuSAP inhibited cell proliferation apparently by irreversibly bundling interphase microtubules (unpublished data), indicating that endogenous NuSAP levels have to be tightly controlled.

It is interesting to note that proteins like NuSAP or TPX2 (Heidebrecht et al., 1997) that show little or no expression in G1 and G0 may be reliable histochemical markers for proliferation and could therefore be useful for cancer prognosis. Consistent with this, we identified NuSAP based on its abundance in proliferating cells, and a significant number of human NuSAP ESTs are derived from cancer tissues. Furthermore, the defects in spindle organization seen in NuSAP-depleted cells could contribute to genomic instability, which is also observed in aggressive tumor cells (Brinkley, 2001).

A role for NuSAP in spindle formation

We used the method of RNA interference knockdown to study the function of NuSAP in cells. NuSAP levels could be efficiently depleted within 24 h, suggesting that cells only needed to exit one mitosis after transfection of the siRNA to severely affect protein levels. The predominant early consequence of NuSAP depletion was a 50% increase of cells arrested in G2-M (Fig. 6). Several aspects of mitotic spindle formation and function were impaired in NuSAP-depleted cells. For example, in >50% of prometaphase cells, chromosome condensation and congression appeared to be delayed or incomplete. Furthermore, the metaphase arrangement of chromosomes often appeared less compact than in normal cells, displaying unaligned chromosomes that indicated a deficiency in chromosome congression or maintenance of a stable metaphase configuration. The bipolar spindles produced in NuSAP-depleted cells showed a reduction in the

content of microtubules in the spindle midzone, suggesting that NuSAP might be involved in the stabilization or production of spindle microtubules associated with chromosomes at the kinetochore and/or at chromosome arms. This is entirely consistent with the localization of NuSAP to chromatin and the spindle midzone.

Despite malformed spindles and misaligned chromosomes, a significant fraction of NuSAP-depleted cells eventually progressed to anaphase and cytokinesis. At these later mitotic stages, the cells also showed striking defects. The central spindles between the separating chromosomes in NuSAP-depleted cells often contained significantly fewer microtubules than in normal anaphase cells. Possibly as a consequence of this weak central spindle, the chromosomes were typically segregated only incompletely and by a much shorter distance than in control cells. Also at cytokinesis, NuSAP-depleted cells frequently failed to cleave between the partially segregated chromosomes, resulting in binucleated cells that also contained additional centrosomes. These binucleate cells were apparently able to enter at least one subsequent cell cycle, as even long after NuSAP suppression, >30% of the cells exhibited multipolar spindles. These spindle poles contained essential structural components like γ-tubulin and NuMA, as well as the centriolar marker centrin. Interestingly, a similar multipolar spindle phenotype has recently been described after suppression of TPX2 (Garrett et al., 2002). However, unlike for TPX2, where multiple poles were suggested to arise from fragmentation of centrosomal material, it is likely that the appearance of multipolar spindles is an indirect consequence of NuSAP suppression. After depleting NuSAP for one cell cycle, only aberrant spindle organization (but no increase in multipolar spindles) was observed. Multipolar spindles arose only much later, and are therefore most likely caused by the observed defects in the preceding round of chromosome segregation and cytokinesis.

Materials and methods

Cell culture and treatments

Murine osteoblast-like MC3T3E1 cells (Sudo et al., 1983) were cultured in MEM supplemented with 10% FCS. Serum starvation–induced growth arrest was accomplished in subconfluent cultures by changing complete medium to medium containing 0.1% FCS. Synchronization of MC3T3E1 cells at S phase was achieved using a double-thymidine block (Stein and Stein, 1990a). COS1 cells were cultured in DME supplemented with 10% FCS, 2 mM L-glutamine, and antibiotics. HeLa cells were cultured in MEM supplemented with 10% FBS and were synchronized using a thymidine block (2 mM for 20 h). The NRK clone stably expressing histone 2B-CFP was obtained, maintained, and synchronized as described previously (Beaudouin et al., 2002). For synchronization using aphidicolin, cells were arrested 1.5 h after transfection. The PtK_2 clone stably expressing human α-tubulin–YFP was a gift from Patrick Keller (Max Planck Institute of Molecular Cell Biology, Dresden, Germany), and was cultured in MEM supplemented with 10% FCS, 2 mM L-glutamine, antibiotics, and 1× nonessential aa.

Cloning of mouse NuSAP cDNA

Total RNA extracted from MC3T3E1 cultures at the stage of proliferation or differentiation (mineralizing) was used in a differential display analysis, which was performed essentially as described previously (Liang et al., 1993). To obtain the full-length cDNA, a 5′-RACE kit (Invitrogen) was used. All PCR products were ligated into the pGEMTEasy cloning vector (Promega) and subsequently sequenced.

Northern blot analysis

Total RNA extracted from cell cultures using TRIzol® LS (Invitrogen) was separated by electrophoresis, transferred to nylon membranes, and hybridized with cDNA probes as follows: pFO002 to detect *histone H4* (Pauli et al., 1989), which was provided by Gary Stein (University of Massachusetts Medical School, Worcester, MA), and a 0.8-kb *NuSAP* BglII/ AspI restriction fragment. To assess equal loading, blots were rehybridized with a radiolabeled *18 S* ribosomal probe.

Construction of NuSAP vectors

The NuSAP-GFP vectors were designed to contain the coding sequences of NuSAP fused upstream to the GFP sequence of the pEGFP-N1 plasmid (CLONTECH Laboratories, Inc.). Specific primers incorporating a 5′ SacI and a 3′ BamHI site were used to obtain the insert. Vectors containing YFP- and CFP-tagged NuSAP were constructed by subcloning the full-length NuSAP cDNA from pNuSAP-EGFP into pEYFP-N1 and pECFP-N1 (CLONTECH Laboratories, Inc.). For construction of the Myc-tagged NuSAP vector, the GFP tag was removed by digesting with BamHI and NotI, and by inserting a Myc adaptor duplex containing these restriction sites. The vector used in the transcription and translation reaction was constructed using XhoI and BamHI restriction fragments derived from the pNuSAP-EGFP vector, which was inserted into the complementary sites of the pcDNA3.1MycHisB plasmid (Invitrogen). The GST-NuSAP-C fusion vector used for protein expression in *Escherichia coli* for antibody generation was designed to contain the COOH-terminal coding sequence (530 bases) of mouse NuSAP fused downstream to the GST sequence of the pGEX5X1 plasmid (Amersham Biosciences). Specific primers incorporating a 5′ BamHI and a 3′ XhoI site were used. The zzNuSAP vector used for recombinant protein expression in the microtubule-binding assay was constructed by amplifying the coding region of NuSAP from pNuSAP-EGFP and cloning into the SphI-BamHI sites of zzpQE80, a derivative of pQE (QIAGEN) with two consecutive z-tags (IgG-binding domain from protein A) at the NH_2 terminus and a COOH-terminal His tag. All constructs were sequenced to verify junctions and to ensure the proper NuSAP sequence.

Recombinant protein expression and purification

zzNuSAP was expressed from zzpQE80 in *E. coli* BL21 Rosetta (Novagen) and purified on Nickel-NTA agarose (QIAGEN). GST and GST-NuSAP-C were expressed from pGEX5X vectors in *E. coli* BL21-Codon Plus (DE3)-RIL (Stratagene).

In vitro transcription and translation

For in vitro NuSAP protein production, plasmid DNA was transcribed and translated using the TNT T7 reticulocyte lysate system (Promega). In the radioactive assays translation grade L-[^{35}S]cysteine (1,000 Ci/ mmol; Amersham Biosciences) was used, and translation products were separated by SDS-PAGE and further processed for fluorography. Luciferase DNA was used as a positive control. Treatment with calf intestine alkaline phosphatase was for 30 min at 37°C. In the nonradioactive assays, protein samples were further processed for Western blot analysis.

Microtubule-binding assay

A nonradioactive crude transcription and translation reaction product was used for the sedimentation assay in the presence and absence of pure, prepolymerized microtubules. The assay was performed using the Microtubule-Associated Protein Spin-Down Assay Biochem kit (Cytoskeleton, Inc.) according to the manufacturer's instructions. Controls that were run included detecting BSA (negative control) and MAP-2 (positive control).

For the direct microtubule-binding assay, 10 μM porcine tubulin, purified according to Mitchison and Kirschner (1984), was incubated with 1 μM purified zzNuSAP in BRB-80 buffer (80 mM Pipes, 1 mM K-EGTA, and 1 mM $MgCl_2$, pH 6.8) containing 2 mM GTP and 20 μM taxol for 20 min at 30°C. The reaction was then centrifuged through a sucrose-BRB-80 cushion at 100,000 *g* for 10 min. Pellet and supernatant were applied to SDS-PAGE, tubulin was detected by Coomassie blue staining, and zzNuSAP was detected by immunoblotting.

Primary antibodies

Rabbit polyclonal anti-$NuSAP_r$ antibodies were generated using purified, bacterially expressed GST fusion (GST-NuSAP-C) as antigen. The antibodies were affinity purified by sequential passage through GST and GST-NuSAP-C fusion protein columns, according to the manufacturer's instructions (GST orientation kit; Pierce Chemical Co.). The polyclonal anti-peptide rabbit antibody (anti-$NuSAP_p$) was generated using a peptide (QENQENQDPRDTAEV) coupled to KLH as antigen in an immunization program performed at Eurogentec. The anti-$NuSAP_p$ serum was affinity purified using antigen peptide coupled to CNBr-activated Sepharose 4B (Amersham Biosciences).

Antibodies were used to detect epitope-tagged NuSAP as follows: anti-c-Myc rabbit antibody (A-14; Santa Cruz Biotechnology, Inc.) and anti-c-Myc mouse mAb (clone 9E10; Sigma-Aldrich). Mouse mAbs were used as follows: anti-α-tubulin (clone DM1A; Sigma-Aldrich), anti-γ-tubulin (clone GTU-88; Sigma-Aldrich), anti-β-actin (clone AC-15; Sigma-Aldrich), anti-BrdU (clone B44; Becton Dickinson), and anti-BSA (clone BSA-33; Sigma-Aldrich). In addition, goat pAbs were used as follows: anti-lamin B (M-20; Santa Cruz Biotechnology, Inc.) and anti-MAP-2 (D-19; Santa Cruz Biotechnology, Inc.). Anti-γ-tubulin rabbit (AK-15; Sigma-Aldrich) antibody was also used. The mouse mAb to nucleolin was provided by Benigno Valdez (Baylor College of Medicine, Houston, TX). The anti-NuMA rabbit antibody was provided by Duane Compton (Dartmouth Medical School, Hanover, NH). The anti-centrin mAb (20H5) was provided by Jeffrey Salisbury (Mayo Clinic, Rochester, MN).

Confocal microscopy, immunofluorescence, and image analysis

For immunostaining of endogenous NuSAP and nucleolin, MC3T3E1 cells were fixed in 1% PFA for 10 min. Images of endogenous NuSAP during mitosis were primarily made using anti-$NuSAP_p$ antibody in cells that were fixed in 0.1% glutaraldehyde (containing 0.5% Triton X-100) for 15 min, followed by a 10-min incubation in 0.5 mg/ml $NaBH_4$ to reduce free aldehyde groups. Anti-$NuSAP_r$ antibody stains weaker in this fixative condition. This fixative was also used to stain Myc-tagged NuSAP in transfected (FuGENE™; Roche) COS1 cells, using anti-c-Myc mouse antibodies (clone 9E10), and to detect incorporated BrdU, which also required the subsequent incubation of cells in 0.07 N NaOH for 2.5 min to denature genomic DNA. Methanol fixation was also used to detect lamin B, centrin, γ- and α-tubulin, NuSAP, and NuMA in MC3T3E1 and HeLa cells.

NuSAP, NuMA, and α-tubulin were also detected in permeabilized MC3T3E1 cells. In the permeabilization assay, cells were first briefly (35 s) incubated in warm (37°C) microtubule-stabilizing PEM buffer (100 mM Pipes, pH 6.9, 5 mM EGTA, and 1 mM $MgCl_2$), then extracted for 30 s in detergent (0.1% Triton X-100)-containing PEM buffer followed by fixation in 1% PFA for 15 min. For extensive permeabilization of transfected COS1 cells, extraction was prolonged to 3 min, and cells were fixed in 0.5% glutaraldehyde.

Further processing included incubating cells in 5% BSA for 10 min before incubations with primary and secondary antibodies for 1 h at RT (diluted in 0.5% Tween 20). Secondary antibodies were conjugated to Alexa®-488 or -546 dye (Molecular Probes, Inc.). Cells were mounted in DakoCytomation mounting medium, containing TO-PRO-3 (Molecular Probes, Inc.) when nucleic acids were stained. Images of fixed cells were acquired on an inverted microscope (Diaphot 300; Nikon) (Plan Apo 60×/1.40 oil) connected to a confocal microscope (model MRC1024; Bio-Rad Laboratories) using LaserSharp software (version 3.2).

The four-dimensional confocal imaging system used has been described elsewhere (Gerlich et al., 2001; Beaudouin et al., 2002). In brief, imaging was performed on a customized microscope (model LSM510; Carl Zeiss MicroImaging, Inc.) equipped with a z-scanning stage, selected PMTs, a 413 nm Kr and 488 nm Ar laser, custom dichroics, and emission filters. Images were acquired using a 63× PlanApochromat NA 1.4 DIC oil immersion objective. Only images from cells that completed mitosis normally were used for subsequent analysis. Images were processed in Adobe Photoshop® version 6.0.1 (Adobe Systems).

RNA interference

For siRNA, the following target sequences in the NuSAP cDNA were used: 5′-AACTGAGATACACGTTAGCAG-3′ and 5′-AAGATCTCTATGCACGGATGA-3′ in the mouse, and 5′-AAGCACCAAGAAGCTGAGAAT-3′ in humans. As a nonspecific control, the GL2 luciferase siRNA duplex was used (Elbashir et al., 2001). Oligonucleotides (Dharmacon Research, Inc.) were annealed and transfected using Oligofectamine™ (Invitrogen) as described previously (Elbashir et al., 2001). Thymidine-synchronized HeLa cells were transfected with the siRNA duplexes 2 h after release. These synchronized cells were analyzed at different time points after transfection (10, 30, and 50 h) corresponding with successive M phases, but complete suppression of NuSAP was only manifest from the second mitosis (30 h after transfection).

Extract preparation and Western blot analysis

Nuclear extracts of MC3T3E1 cells were prepared essentially as described by Feng et al. (2000). Whole-cell extracts were prepared from the different cell lines, by washing and scraping cells in PBS containing 5 mM EDTA and 5 mM EGTA, and subsequently lysing cell pellets in ice-cold TCL buffer (50 mM TrisCl, pH 8.0, 150 mM NaCl, 0.1% SDS, 1% NP-40, and 0.5% sodium deoxycholate) containing protease inhibitors. Lysed cells were subsequently sonicated for 5 s and centrifuged at 14,000 *g* (20 min at 4°C). Proteins were boiled in SDS sample buffer, separated by SDS-PAGE using precast 4–12% Bis-Tris gels (Invitrogen), and transferred to nitrocellulose membranes (Amersham Biosciences). Membranes were probed and subsequently developed by ECL (Western Lightning; Perkin Elmer).

FACS® analysis

Subconfluent MC3T3E1 and HeLa cells were stained with propidium iodide and subsequently analyzed for DNA content on a FACScan™ (Becton Dickinson) flow cytometer using CellQuest™ software (BD Biosciences).

We gratefully acknowledge the following scientists, who provided key materials: Duane Compton, Patrick Keller, Jeffrey Salisbury, Gary Stein, Benigno Valdez. We are also grateful to Victor Van Duppen for assistance with the FACS® analysis. We wish to thank Iain Mattaj and his group for stimulating discussions.

This work was supported by the 'Fonds voor Wetenschappelijk Onderzoek' (FWO; G.0233.97), and European Commission Transnational Access to Research Infrastructures Programme (European Advanced Light Microscopy Facility at the EMBL in Heidelberg) grants, and a long-term EMBO fellowship (to K. Ribbeck). J. Beaudouin was supported by a fellowship through EMBL's International Ph.D. Program; J. Ellenberg acknowledges funding from the Human Frontiers Science Program (RGP0031/2001-M).

Submitted: 21 February 2003
Accepted: 29 July 2003

References

Aravind, L., and E.V. Koonin. 2000. SAP - a putative DNA-binding motif involved in chromosomal organization. *Trends Biochem. Sci.* 25:112–114.

Beaudouin, J., D. Gerlich, N. Daigle, R. Eils, and J. Ellenberg. 2002. Nuclear envelope breakdown proceeds by microtubule-induced tearing of the lamina. *Cell.* 108:83–96.

Brinkley, B.R. 2001. Managing the centrosome numbers game: from chaos to stability in cancer cell division. *Trends Cell Biol.* 11:18–21.

Compton, D.A., I. Szilak, and D.W. Cleveland. 1992. Primary structure of NuMA, an intranuclear protein that defines a novel pathway for segregation of proteins at mitosis. *J. Cell Biol.* 116:1395–1408.

Dasso, M. 2001. Running on Ran: nuclear transport and the mitotic spindle. *Cell.* 104:321–324.

Drewes, G., A. Ebneth, and E.M. Mandelkow. 1998. MAPs, MARKs and microtubule dynamics. *Trends Biochem. Sci.* 23:307–311.

Elbashir, S.M., J. Harborth, W. Lendeckel, A. Yalcin, K. Weber, and T. Tuschl. 2001. Duplexes of 21-nucleotide RNAs mediate RNA interference in cultured mammalian cells. *Nature.* 411:494–498.

Feng, X., S.L. Teitelbaum, M.E. Quiroz, S.L. Cheng, C.F. Lai, L.V. Avioli, and F.P. Ross. 2000. Sp1/Sp3 and PU.1 differentially regulate beta(5) integrin gene expression in macrophages and osteoblasts. *J. Biol. Chem.* 275:8331–8340.

Gaglio, T., M.A. Dionne, and D.A. Compton. 1997. Mitotic spindle poles are organized by structural and motor proteins in addition to centrosomes. *J. Cell Biol.* 138:1055–1066.

Garrett, S., K. Auer, D.A. Compton, and T.M. Kapoor. 2002. hTPX2 is required for normal spindle morphology and centrosome integrity during vertebrate cell division. *Curr. Biol.* 12:2055–2059.

Gerlich, D., J. Beaudouin, M. Gebhard, J. Ellenberg, and R. Eils. 2001. Four-dimensional imaging and quantitative reconstruction to analyse complex spatiotemporal processes in live cells. *Nat. Cell Biol.* 3:852–855.

Gruss, O.J., R.E. Carazo-Salas, C.A. Schatz, G. Guarguaglini, J. Kast, M. Wilm, N. Le Bot, I. Vernos, E. Karsenti, and I.W. Mattaj. 2001. Ran induces spindle assembly by reversing the inhibitory effect of importin alpha on TPX2 activity. *Cell.* 104:83–93.

Gruss, O.J., M. Wittmann, H. Yokoyama, R. Pepperkok, T. Kufer, H. Sillje, E. Karsenti, I.W. Mattaj, and I. Vernos. 2002. Chromosome-induced microtubule assembly mediated by TPX2 is required for spindle formation in HeLa cells. *Nat. Cell Biol.* 4:871–879.

Haren, L., and A. Merdes. 2002. Direct binding of NuMA to tubulin is mediated by a novel sequence motif in the tail domain that bundles and stabilizes microtubules. *J. Cell Sci.* 115:1815–1824.

Heald, R., R. Tournebize, T. Blank, R. Sandaltzopoulos, P. Becker, A. Hyman, and E. Karsenti. 1996. Self-organization of microtubules into bipolar spindles around artificial chromosomes in Xenopus egg extracts. *Nature.* 382:

420–425.

Heidebrecht, H.J., F. Buck, J. Steinmann, R. Sprenger, H.H. Wacker, and R. Parwaresch. 1997. p100: a novel proliferation-associated nuclear protein specifically restricted to cell cycle phases S, G2, and M. *Blood.* 90:226–233.

Hetzer, M., O.J. Gruss, and I.W. Mattaj. 2002. The Ran GTPase as a marker of chromosome position in spindle formation and nuclear envelope assembly. *Nat. Cell Biol.* 4:E177–E184.

Jakel, S., J.M. Mingot, P. Schwarzmaier, E. Hartmann, and D. Gorlich. 2002. Importins fulfil a dual function as nuclear import receptors and cytoplasmic chaperones for exposed basic domains. *EMBO J.* 21:377–386.

Joshi, H.C., M.J. Palacios, L. McNamara, and D.W. Cleveland. 1992. Gamma-tubulin is a centrosomal protein required for cell cycle-dependent microtubule nucleation. *Nature.* 356:80–83.

Kahana, J.A., and D.W. Cleveland. 1999. Beyond nuclear transport. Ran-GTP as a determinant of spindle assembly. *J. Cell Biol.* 146:1205–1210.

Kahana, J.A., and D.W. Cleveland. 2001. Cell cycle: Some importin news about spindle assembly. *Science.* 291:1718–1719.

Karsenti, E., and I. Vernos. 2001. The mitotic spindle: a self-made machine. *Science.* 294:543–547.

Lewis, S.A., I.E. Ivanov, G.H. Lee, and N.J. Cowan. 1989. Organization of microtubules in dendrites and axons is determined by a short hydrophobic zipper in microtubule-associated proteins MAP2 and tau. *Nature.* 342:498–505.

Liang, P., L. Averboukh, and A.B. Pardee. 1993. Distribution and cloning of eukaryotic mRNAs by means of differential display: refinements and optimization. *Nucleic Acids Res.* 21:3269–3275.

Merdes, A., and D.W. Cleveland. 1997. Pathways of spindle pole formation: different mechanisms; conserved components. *J. Cell Biol.* 138:953–956.

Mitchison, T., and M. Kirschner. 1984. Microtubule assembly nucleated by isolated centrosomes. *Nature.* 312:232–237.

Nachury, M.V., T.J. Maresca, W.C. Salmon, C.M. Waterman-Storer, R. Heald, and K. Weis. 2001. Importin beta is a mitotic target of the small GTPase Ran in spindle assembly. *Cell.* 104:95–106.

Pauli, U., J.F. Chiu, P. Ditullio, P. Kroeger, V. Shalhoub, T. Rowe, G. Stein, and J. Stein. 1989. Specific interactions of histone H1 and a 45 kilodalton nuclear protein with a putative matrix attachment site in the distal promoter region of a cell cycle-regulated human histone gene. *J. Cell. Physiol.* 139:320–328.

Peter, M., J. Nakagawa, M. Doree, J.C. Labbe, and E.A. Nigg. 1990. Identification of major nucleolar proteins as candidate mitotic substrates of cdc2 kinase. *Cell.* 60:791–801.

Pfleger, C.M., and M.W. Kirschner. 2000. The KEN box: an APC recognition signal distinct from the D box targeted by Cdh1. *Genes Dev.* 14:655–665.

Rechsteiner, M., and S.W. Rogers. 1996. PEST sequences and regulation by proteolysis. *Trends Biochem. Sci.* 21:267–271.

Stein, G.S., and J.L. Stein. 1990a. Cell synchronization. *In* Cell Growth and Division: A Practical Approach. R. Baserga, editor. IRL Press at Oxford University Press, Oxford. 133–137.

Stein, G.S., J.B. Lian, and T.A. Owen. 1990b. Relationship of cell growth to the regulation of tissue-specific gene expression during osteoblast differentiation. *FASEB J.* 4:3111–3123.

Sudo, H., H.A. Kodama, Y. Amagai, S. Yamamoto, and S. Kasai. 1983. In vitro differentiation and calcification in a new clonal osteogenic cell line derived from newborn mouse calvaria. *J. Cell Biol.* 96:191–198.

Takemura, R., S. Okabe, T. Umeyama, Y. Kanai, N.J. Cowan, and N. Hirokawa. 1992. Increased microtubule stability and alpha tubulin acetylation in cells transfected with microtubule-associated proteins MAP1B, MAP2 or tau. *J. Cell Sci.* 103:953–964.

Wiese, C., A. Wilde, M.S. Moore, S.A. Adam, A. Merdes, and Y. Zheng. 2001. Role of importin-beta in coupling Ran to downstream targets in microtubule assembly. *Science.* 291:653–656.

Wittmann, T., M. Wilm, E. Karsenti, and I. Vernos. 2000. TPX2, A novel xenopus MAP involved in spindle pole organization. *J. Cell Biol.* 149:1405–1418.

Wittmann, T., A. Hyman, and A. Desai. 2001. The spindle: a dynamic assembly of microtubules and motors. *Nat. Cell Biol.* 3:E28–E34.

Yang, C.H., E.J. Lambie, and M. Snyder. 1992. NuMA: an unusually long coiled-coil related protein in the mammalian nucleus. *J. Cell Biol.* 116:1303–1317.